DOI: 10.1016/j.buildenv.2018.05.042

Active control of sound through full-sized open windows

Bhan Lam[1]

Digital Signal Processing Lab, School of Electrical and Electronic Engineering, Nanyang Technological University, Singapore

Chuang Shi

School of Information and Communication Engineering, University of Electronic Science and Technology of China, Chengdu, Sichuan, China

Dongyuan Shi

Digital Signal Processing Lab, School of Electrical and Electronic Engineering, Nanyang Technological University, Singapore

Woon-Seng Gan

Digital Signal Processing Lab, School of Electrical and Electronic Engineering, Nanyang Technological University, Singapore

Submited on 20th Feb 2018, Accepted on 18th May 2018, Available online on 23rd May 2018.

[1] Electronic mail: blam002@e.ntu.edu.sg; Postal Address: Digital Signal Processing Lab, School of Electrical and Electronic Engineering, Nanyang Technological University, Singapore 639798, Singapore

Abstract

There is a pressing need to address urban sustainability challenges of increasing ambient temperatures and noise levels in densely-populated, high-rise cities. Solutions that utilise active noise control on open windows to reduce indoor noise levels seem promising, as natural ventilation is still maintained. Active noise control utilizes acoustic transducers arranged around the open window to generate a secondary incidence noise that destructively interferes with the real noise. The two most common techniques of transducer arrangement, distributed and boundary layouts, are investigated for the typical single-glazed sliding window. Finite element method is used to establish the control performance of the active noise control system and the passive attenuation provided by the sliding window. Based on the investigated fundamental limits of active control, the distributed layout has consistently yielded better performance than the boundary layout. The distributed-layout method can also reduce noise more effectively than a fully-glazed window. Moreover, sources distributed only in the partial opening of a simulated sliding window can attenuate noise as effectively as the fully-glazed window. The distributed-layout method is tested on a full-sized window, where the active control system has up to 16 channels and evenly distributed across the window opening. In the test with tonal sounds, the feasibility of the active control system is demonstrated. The experimental results have validated the simulation findings for normal incidence plane waves.

Keywords: Active Noise Control, Finite Element Method, Noise Mitigation Through Open Windows, Building Acoustics

1 Introduction

Noise pollution is a pressing urban sustainability challenge for urban planners. Increasing urbanisation of the global population has driven common dwellings into high-rise buildings. This creates a dilemma between convenience and noise exposure as planners must decide the proximity of transport infrastructure (the noise source) to the housing estates. Noise barriers, a common noise mitigation measure in densely populated high-rise cities, only partially alleviate the noise problem as they inadvertently diffract noise to the upper floors of nearby high-rise buildings.

Therefore, there is an increasing need in controlling noise at the receiver end, such as noise that propagates through window openings. Furthermore, the importance of natural ventilation as a sustainable solution for rising ambient temperatures, has increased the demand for noise mitigation measures that retain maximum natural ventilation.

Passive noise control techniques have been proposed to increase the noise insulation performance of common single-glazed windows. Kang investigated the use of staggered panels with louvers (lined with micro-perforated absorbers) in between the panels. The performance of the staggered panels outperformed the closed single glazed windows, while allowing some natural ventilation, and without obstructing daylight [1]. Tong et al. also adopted the staggered panel "plenum" window approach and completed a full-scale field study yielding a maximum of 9.5 dB of insertion loss [2,3], albeit at a cost of reduced airflow. Huang et al. improved the noise reduction performance of the staggered panel system to 12 dB, by adopting a hybrid active and passive noise control system [4,5]. To combat noise pollution due to vehicle powertrain noise, Lee et al. proposed an experimental louver system based on the sonic crystal concept and reported a maximum insertion loss of 7.7 dB at 1100 Hz [6].

The passive and hybrid solutions, however, propose heavy modifications that changes the functionality of common single-glazed window systems. Furthermore, the natural ventilation airflow rates can be reduced by up to 2 – 4 times [4]. Hence, noise control strategies that retain maximum natural ventilation are key to meeting urban sustainability challenges. Moreover, noise mitigation strategies that augment onto existing windows can be easily removed when the noise has been mitigated at the source (e.g., better traffic management, completed construction projects, etc.).

To retain airflow rates of common single-glazed windows, several active noise control systems for open windows have been developed. Active noise control (ANC) systems are based on the principle of wave superposition, and thus require transducers (e.g., loudspeakers) that actively interfere (destructively) with the noise wave to achieve reduction. The ANC systems introduced will be grouped by their source arrangement strategies, namely, boundary and distributed layout methods.

Boundary layout ANC systems aim to minimise the physical obstructions in the opening of the window by distributing the control sources on the boundary, i.e., perimeter of the window. For instance, Kwon and Park, placed 8 control sources around the perimeter of a 900 cm^2 (30×30 cm^2) window in a scaled-down mock up, and achieved global control of up to 10 dB in the room interior [7]. The elaborate setup, however, warrants further investigation for scaling to full-sized windows. Although real-time adaptive systems mounted on tilt [8] and sliding windows [9] have been developed recently, control is only effective from 100 to 300 Hz with a 2110 cm^2 (56×142 cm^2, 2° tilt, 5 cm gap) and 225 cm^2 (13×75 cm^2, sliding) opening, respectively. Recent advancements in boundary layout ANC systems on a partially opened regular tilt window (910×910 cm^2) yielded up to 13 dB of control between 100 to 800 Hz, albeit with large transducers ($\varnothing 8$ cm) [10].

In comparison, distributed layout ANC systems are designed to achieve global noise attenuation in the room by arranging control sources within the aperture. Murao and Nishimura demonstrated a real-time ANC system with 4-channels on a 625 cm^2 (25×25 cm^2) square opening, achieving broadband attenuation of 10 dB from 0.5 to 1.5 kHz [11,12]. A virtual sound barrier (VSB) developed for a baffled rectangular opening also utilises the distributed control strategy [13,14]. The VSB system consists of 6 control sources distributed uniformly over the 2881 cm^2 (43×67 cm^2) aperture. Although the VSB was intended for frequencies below 500 Hz, broadband attenuation of up to 20 dB was achieved for a relatively large opening. The prior work mentioned thus far is summarised in Table 1.

Through recent developments, the apparent advantage of distributed over boundary layout ANC systems lie in their scalability. With the same number of sources, the upper frequency limit after which performance is poor, is lower in boundary layout than the distributed layout [15]. Since the control of diffraction around the edges of the aperture become less important as the wavelength decreases relative to the size of the aperture, the attenuation performance of the boundary layout will degrade as the aperture increases [16].

Since existing distributed control ANC studies have focused on the control of noise through unobstructed apertures of limited size, this paper will focus on typical full-sized single-glaze sliding windows as they are prevalent throughout the world. Firstly, as a benchmark for active control performance, the passive attenuation of the single-glaze sliding window is determined for increasing aperture sizes to mimic the mechanism of regular sliding windows. Secondly, using a single channel system, the physical limits of active control are compared numerically under different degrees of window glazing between the distributed and boundary layout. The comparison aims to investigate the limits of a proposed boundary layout [9,17] against the suggested positioning of active control sources away from the wall edges [18]. Thirdly, to quantify the physical limitations of a multichannel distributed layout active control system

DOI: 10.1016/j.buildenv.2018.05.042

Table 1: Summary of prior work in the active control of sound through apertures

Author	Layout	Type	Window Dimensions (W×H cm^2)	Opening Size (cm^2)	No. of Control Sources	Type of Noise	Reduction (Global/Local)
Window							
Murao 2012 [11]	Distributed	Open Aperture	25 × 25	25 × 25	4	BLWN (0.5 to 2kHz)	10-15 dB (Global)
Kwon 2013 [7]	Boundary	Open Aperture	30 × 30	30 × 30	8	BLWN (0.4 to 1 kHz)	Up to 10 dB (Global)
Paimes 2014 [8]	Boundary	Tilt Window (Hopper)	56 × 142	5cm Gap 2° Tilt	Not stated	Real aircraft pass-by (0.2 to 0.16 kHz)	3 dB (Global)
Carme 2016 [9]	Boundary	Sliding Window	75 × 75	13 × 75	5	Traffic Noise (<300 Hz)	15.5 dB (Not Stated)
Hanselka 2016 [10]	Boundary	Tilt Window (Hopper)	91 × 91	Not stated	8	BLWN (0.1 to 1 kHz)	13 dB (Local)
Opening of baffled rectangular cavity							
Wang 2015, 2016 [13,14]	Distributed	Open Aperture	-	43 × 67	6	BLWN (<0.5 kHz)	~15 dB (Global)
Wang 2017 [19]	Boundary	Open Aperture	-	43 × 67	8	BLWN (<1 kHz)	10 dB (Local, 0.2 m around error points)
Wang 2017 [19]	Boundary	Open Aperture	-	43 × 67	32	Tonal (<1 kHz)	~20dB (Global)
Wang 2017 [19]	Distributed	Open Aperture	-	43 × 67	32	Tonal (<1 kHz)	~20dB (Global)

implemented on the sliding window, the control performance is investigated numerically for the full-range of noise incidence angles. Lastly, the feasibility of a real-time distributed-layout ANC system is investigated on a full-sized two-panel sliding window. The size of the simulation model closely models the experimental setup for direct comparisons.

2 Acoustic considerations

The global effectiveness of ANC for windows treats the open aperture as the noise source to be controlled. At frequencies where the wavelengths are much smaller than the size of the aperture, the control problem approximates the free-field condition [20] and thus, the distributed control strategy should be used over the boundary technique. Intuitively, this implies that when the wavelengths are large compared to the aperture size, relatively few sources are required, suggesting that the boundary layout can provide effective control. On the contrary, the influence of diffraction becomes important at large wavelengths and has been shown to substantially limit the performance of configurations with few sources distributed across the aperture as well as along the boundary [16,18,20].

Moreover, as the noise incidence angle increases, the number of control sources must increase to maintain the same attenuation performance. This relation arises from the inverse relationship of the minimal separation distance between the sources, and $1 + \sin\theta$, where θ is the angle of noise incidence [16,18,20].

Although the analytical solution indirectly suggests that the attenuation performance of the boundary control strategy will degrade in proportion to an increase in aperture size; the influence of diffraction through the aperture in a rigid wall, and the practicality of the boundary control strategy warrants further investigation.

3 Numerical Study

3.1 Passive insulation of single-glazed windows

Sound insulation provided by a tightly-sealed, 6 mm thick, single-glazed window is a reasonable benchmark to grade the attenuation performance of open window active control systems. The 2D finite element method (FEM) simulation is set up to determine the transmission loss of a fully glazed window, as shown in Figure 1(a). The noise source is initiated as a background plane wave that is travelling in the x-axis direction when incidence angle θ is 0°. For consistency and accuracy, the minimum element size is fixed at one-sixth the wavelength of 4000 Hz. A far-field arc with 1100 evenly distributed discrete points encompasses the entire window opening to monitor the attenuation performance of the active control system.

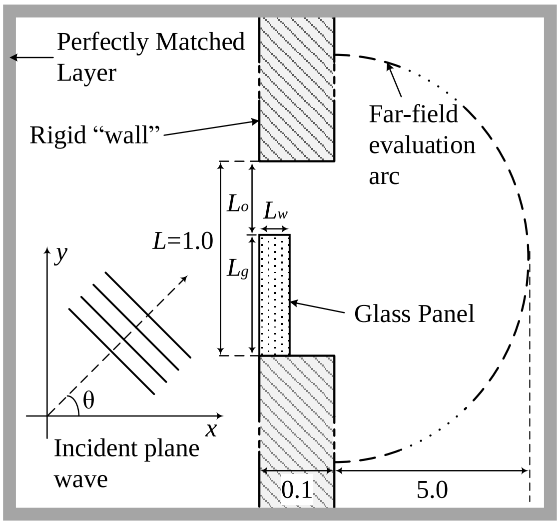

(a)

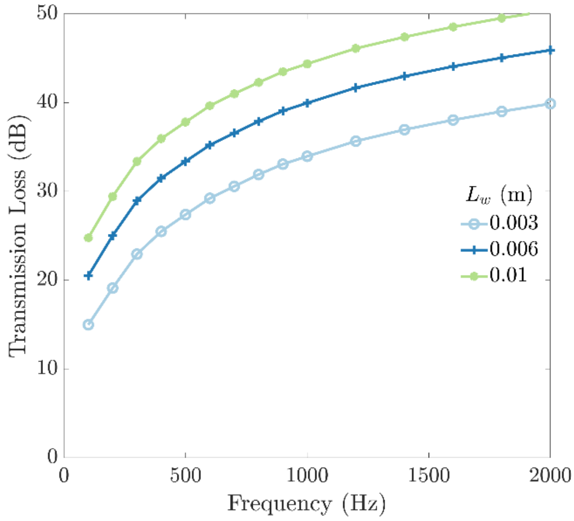

(b)

Figure 1: (a) FEM simulation model to determine transmission loss. With all units in m. (b) Transmission loss $TL_{GR=1}$ of a fully-glazed glass panel with different thickness, L_w m, at 0° noise incidence.

The transmission loss (TL) is calculated by evaluating the sum-of-the-squared pressures on a far-field arc, written as

$$TL_{GR} = 10\log_{10}\frac{\mathbf{p}_{L_g}^{\mathrm{H}}\mathbf{p}_{L_g}}{\mathbf{d}^{\mathrm{H}}\mathbf{d}}, \tag{1}$$

where $\mathbf{d}$ is vector of complex pressure values at the arc without the glass panel, $\mathbf{p}_{L_g}$ is the vector of complex pressure values at the arc when the glass is L_g m, superscript $^{\mathrm{H}}$ is the Hermitian operator, and $GR = L_g/L$ is the glazing ratio.

Transmission loss due to passive insulation of a sealed window is emulated with a glass panel spanning the entire aperture and a thickness of L_w m, as shown in Figure 1(b). From the simulation with a plane wave at 0° incidence, the full glazing performance $TL_{GR=1}$ increases uniformly across all frequencies as thickness L_w increases. Performance decreases rapidly with increasing wavelength, when the wavelength is larger than the size of the aperture, L m. Results from the FEM simulation for $L_w = 0.003$ m agrees with the measured data from past experiments using the reverberation chamber method as described in ISO 10140 [21–24]. To form a basis of comparison to the full-scale model, the size of the aperture is fixed at $L = 1.0$ m for all FEM simulations in this study. The thickness L_w is fixed at 6 mm from this point forth, as the thickness of 6 mm is commonly used in single panel windows in Singapore and Hong Kong [3].

The transmission loss of the fully-glazed aperture $TR_{GR=1}$ increases with increasing frequency, as shown in Figure 2. TL_{GR} degrades drastically as a function of frequency once the glazing ratio is less than 100%. As GR decreases, the attenuation performance degrades uniformly across all frequencies, as shown in Figure 2. It is worth noting that passive attenuation is still notable (more than 5 dB) and uniform across all frequencies for glazing ratio

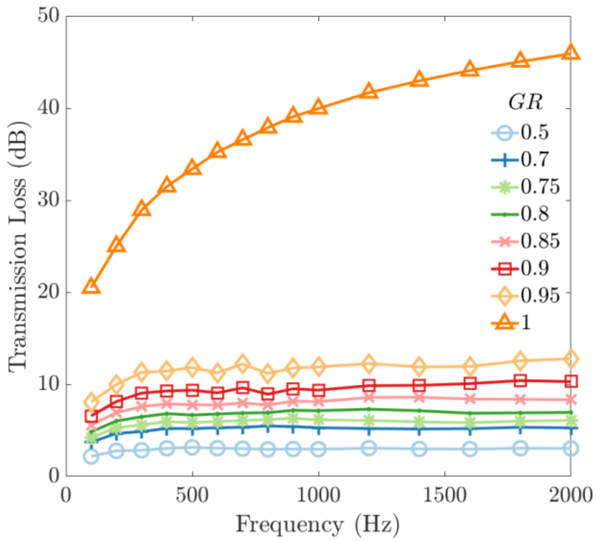

Figure 2: Transmission loss TL_{GR} for different GR, with glass thickness of $L_w = 0.006$ m, at 0° noise incidence.

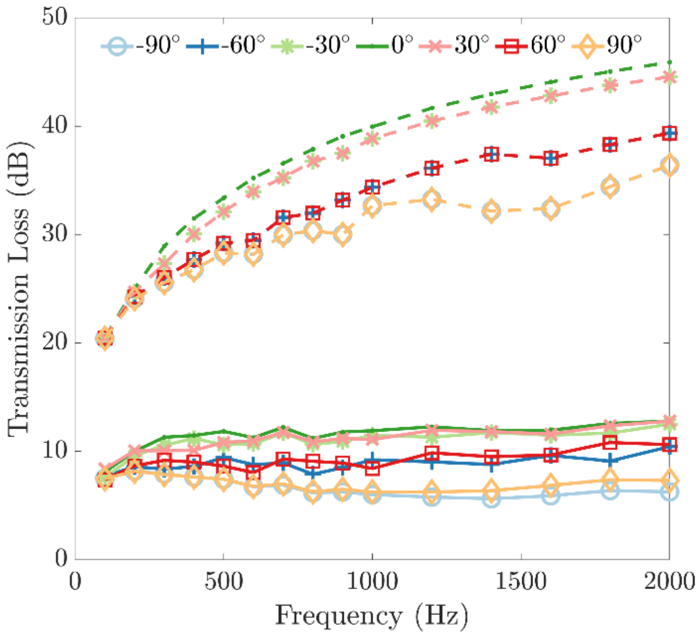

Figure 3: Transmission loss at full-glazing $TL_{GR=1}$ (dashed line), and 95% glazing, $TL_{GR=0.95}$ (solid line), at different noise incidence angles.

between 75% and 95%. The reduced attenuation of the window panel at frequencies 300 Hz and below also presents a complementary role for an ANC system to provide increased attenuation, as demonstrated by Carme et al [17].

When the plane wave incidence angle is varied from -90° to 90°, the attenuation performance for all GR degrades with increasing angle of incidence as a function of frequency, as shown in Figure 3. There is no notable difference in performance between the positive and corresponding negative noise incidence angles, as shown in Figure 3.

3.2 Active control formulation

The active control system is evaluated using the simulation setup shown in Figure 1(a). For a global control formulation, the sound power transmitted through the aperture is controlled by minimising the sum-of-the-squared pressures at the same 1100 discrete points on the far-field arc depicted in Figure 1(a). Hence, the optimal solution of the control problem is obtained by minimising a cost function [25], which is the sum of modulus squared error signals, denoted here as a vector $\mathbf{e}$ containing 1100 elements, and is given by

$$\mathbf{e} = \mathbf{d} + \mathbf{Gu}, \tag{2}$$

where $\mathbf{d}$ and $\mathbf{Gu}$ are vectors of complex pressures due to the disturbance noise only, and from contributions of all the N control sources, respectively. $\mathbf{G}$ is the matrix of complex plant responses and $\mathbf{u}$ is the vector of control source strengths, at all the evaluation points on the evaluation arc. The cost function to be minimised is therefore given by

$$J = \mathbf{e}^{\mathrm{H}}\mathbf{e} = \mathbf{q}_s^{\mathrm{H}}\mathbf{A}\mathbf{q}_s + \mathbf{q}_s^{\mathrm{H}}\mathbf{b} + \mathbf{b}^{\mathrm{H}}\mathbf{q}_s + \mathbf{d}^{\mathrm{H}}\mathbf{d}, \tag{3}$$

where $\mathbf{A} = \mathbf{G}^{\mathrm{H}}\mathbf{G}$ and $\mathbf{b} = \mathbf{G}^{\mathrm{H}}\mathbf{d}$, $\mathbf{q}_s$ is the vector of control sources. The vector of optimal secondary source strengths is derived from equating the derivative of (3) to zero yielding

$$\mathbf{q}_s = -(\mathbf{G}^{\mathrm{H}}\mathbf{G} + \beta\mathbf{I})^{-1}\mathbf{G}^{\mathrm{H}}\mathrm{d}, \tag{4}$$

where β is the regularisation or weighting parameter that limits the control effort to minimise overdriven control sources without increasing the residual mean-square error [25].

Similar to the transmission loss defined in Eq. (1), the transmission loss of the active control system can be written as

$$TL_{GR,ANC} = -10\log_{10}\frac{\mathbf{e}^{\mathrm{H}}\mathbf{e}}{\mathbf{d}^{\mathrm{H}}\mathbf{d}}, \tag{5}$$

where GR is the glazing ratio, $\mathbf{e}$ is the vector of complex pressure values after active control as defined by Eq. (2), and $\mathbf{d}$ is the vector of complex pressure values of the fully open aperture ($L_g = 0$ m) as defined in Eq. (1).

DOI: 10.1016/j.buildenv.2018.05.042

3.3 Performance of the single source ANC system

In the 2D FEM model used, the simulated point source (denoted by cross mark), is essentially an incoherent line source that radiates cylindrical waves [26]. Hence, a single point source on the 2D model is a cross-sectional view of a line source. For simplicity, the acoustic line source represented with a cross mark will henceforth be referred to as an individual ‘point’ source.

Due to the unique setup of the common sliding window in France, an active control system was developed to mitigate urban noise transmission through an open window with minimal modifications to existing windows [9,17]. The control sources were placed along the edge of one wall, with the speakers facing perpendicular to the aperture, understandably for aesthetical

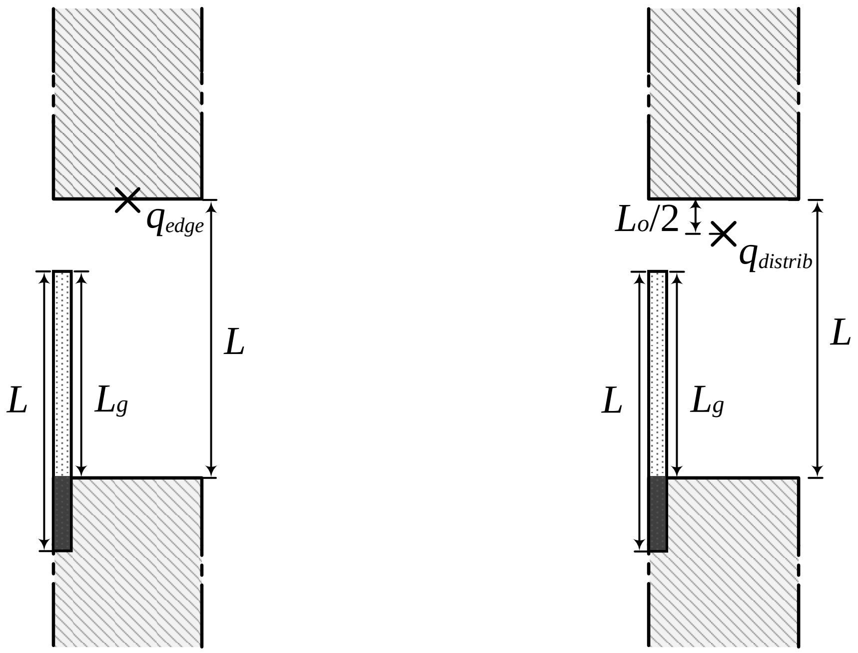

(a) (b)

Figure 4: A close-up view of the aperture showing positions of a single source for (a) the single-sided boundary layout denoted by a cross-mark along the edge of the wall width, q_{edge}, and (b) for the proposed distributed layout located $0.125/2 = 0.0625$ m away from the edge denoted by $q_{distrib}$. Both line sources are placed in the middle of the wall width, and the shaded area indicates part of the glass panel that has been occluded and is included for illustrative purposes.

reasons. This single-sided source layout can be classified as a form of boundary control strategy. However, it was previously found that placing sources on the edge significantly limits the performance of an active control system in the open aperture scenario albeit for a relatively large number of sources [18].

As there is a lack of analysis on the physical limits of the discussed single-sided boundary control in [9,17], it is numerically investigated here with comparisons to a proposed distributed strategy. The single-sided boundary control strategy, and a proposed single source 'distributed' system is evaluated in 2D FEM as depicted in Figure 4(a) and (b), respectively. Since the glass panel is based on the same model shown in Figure 1(a) as sliding downwards in the depicted cross-sectional top view, the single sources are positioned near the top wall, where the opening caused by the downwards sliding glass panel will start (i.e., L_g decreases). Hence, the single-sided boundary control is represented by a source located on the wall edge, denoted by q_{edge} in Figure 4(a). The distributed layout is represented by a single source located $0.125/2 = 0.0625$ m away from the edge of the wall, denoted by $q_{distrib}$ in Figure 4(b). Both the single line sources are located in the middle of the wall width, based on recommendations from a previous study about the physical limits of active control of noise through an aperture [18].

The parameter L_o, is the aperture size of the acoustic window system described in [17], which is based on the maximum window gap for infant safety in France. For the convenience of experimentation and execution of the simulations, L_o is reduced to 12.5 cm instead of 13 cm. Hence, the line source placed at $L_o/2 = 0.0625$ m, which is the centre of the intended opening in [17].

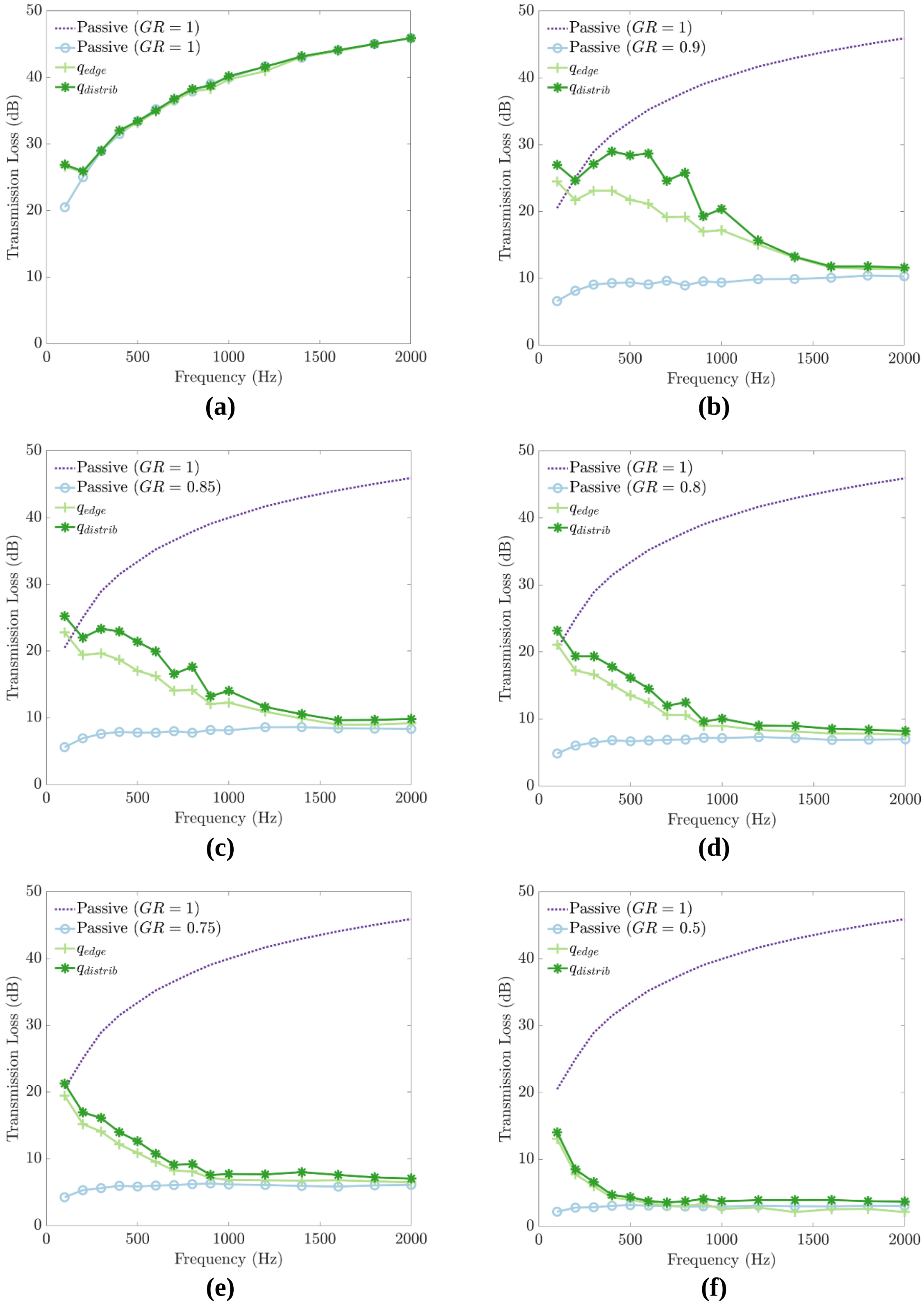

Figure 5: Transmission loss $TL_{GR,ANC}$ of the single line source systems q_{edge} and $q_{distrib}$, with GR equals (a) 1, (b) 0.9, (c) 0.85, (d) 0.8, (e) 0.75, (f) and 0.5. Passive TL_{GR} and $TL_{GR=1}$ included for comparison.

3.3.1 Performance of single source ANC system at normal incidence

Besides investigating the difference in performance between the two strategies with the intended window gap size of L_o ($GR = 0.875$), it is also worthwhile to explore the changes in performance with decreasing GR (i.e., increasing gap size). By varying GR between 1 (full-glazing) and 0.5 (fully-open two-panel sliding window), the physical limits of the single line source system will be defined in the context of the regular operating conditions of a two-panel sliding window. The performance limits of q_{edge} and $q_{distrib}$ are firstly determined for noise impinging at normal incidence, with decreasing L_g.

At full-glazing ($GR = 1$), the single source in both configurations are not contributing to the transmission loss of the window system except at 100 Hz, as illustrated in Figure 5(a). When the glazing ratio is close to the limit of the proposed system in [17], the arrangement where the single source is located slightly away from the wall ($q_{distrib}$) outperforms the boundary layout (q_{edge}) by as much as 8 dB, as shown in Figure 5(b) and (c). Even at GR beyond the effective range of a single source system, the benefit of placing the sources (which even becomes arbitrary when $(L - L_g) \neq L_o$) away from the edge of the wall (i.e., $q_{distrib}$) is apparent, as illustrated in Figure 5(d) and (e).

If the goal of active control is to attain the passive attenuation level of the fully-glazed aperture, whilst still allowing natural ventilation ($GR < 1$), the results presented in this subsection also illustrates that a single source (or line of sources as depicted in [17]) is insufficient.

3.3.2 Performance of single source ANC system at oblique incidences

It may seem intuitive that placing the source on the edge (i.e., q_{edge}) might be beneficial for noise impinging from oblique angles, especially for controlling the diffracted waves near the

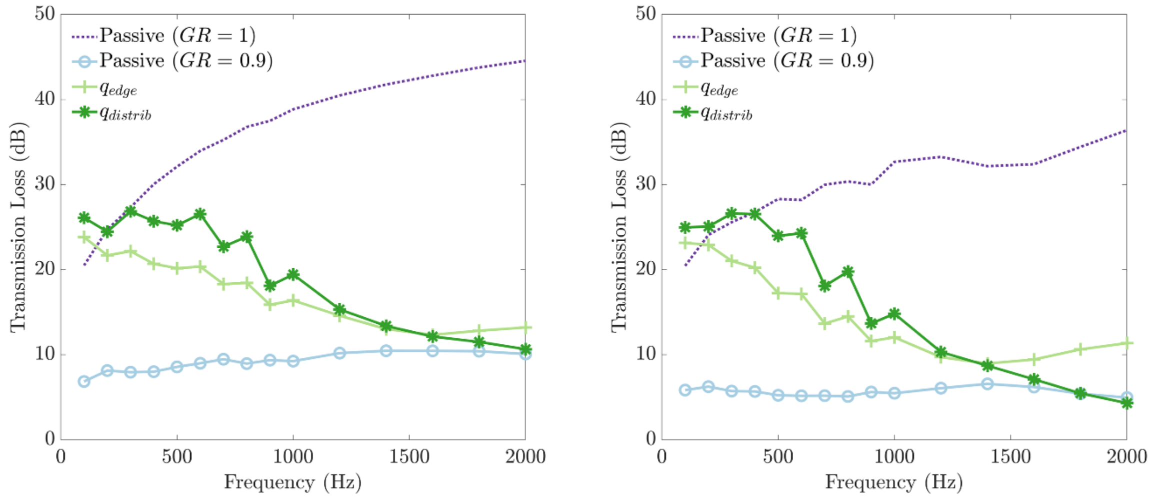

(a) (b)

Figure 6: Transmission loss of the single source ANC system, $TL_{0.9,ANC}$, as a function of frequency for source positions at q_{edge} and $q_{distrib}$, when noise incidence angles are (a) 30°, and (b) 90°. Transmission loss of the fully glazed window, TL_1, and with 90% glazing, $TL_{0.9}$, without ANC is included for comparison.

edges. However, it has been also been shown to be otherwise in a multichannel layout, where placing active control sources away from the edge provided better attenuation performance at obliques incidences as described in section 3.3.1 [18].

Hence, the same single channel setup from section 3.3.1 is used to investigate the performance of the single source system by varying the angle of noise incidence from -90º to 90º in steps of 30º. In all the cases simulated, $q_{distrib}$ always outperforms q_{edge} for frequencies less than 1000 Hz. The scenario when $GR = 0.9$, with noise impinging from 30º and 90º is shown in Figure 6 (a) and (b) respectively.

From the comparison between the attenuation performance of q_{edge} and $q_{distrib}$, it is now clear that even for a single source, it should not be positioned on the edge of the wall. However, at

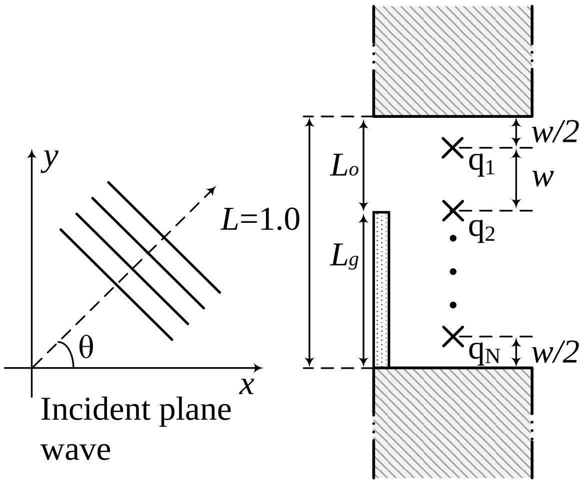

Figure 7: Arrangement of secondary sources within the aperture, relative to the position of the glass panel.

present, the physical basis for this phenomenon is still unclear, owing to known complexities of the diffracted sound field in the aperture [27].

In gist, the numerical analysis into the physical limits of an acoustic window system using a single-sided boundary layout [9] has revealed that a single source is unable to attain sufficient attenuation regardless of GR and θ. Furthermore, one should avoid positioning sources on the edge when scaling the number of sources used, as shown in this section and in a previous study [18].

3.4 Performance of a distributed-layout multichannel ANC system

In the distributed control system, the control sources are symmetrically distributed across the entire opening, where sources are spaced $w = L \,/\, N$ m apart with peripheral sources $w \,/\, 2\ \mathrm{m}$ away from the wall, as depicted in Figure 7. The minimum number of sources required in the aperture can be guided by the spatial aliasing formula in microphone array processing, given by $kw < 2\pi \big/ (\sin\theta + 1)$, where k is the wavenumber, from a previous study [18,28] and from a free-field analysis [16,20].

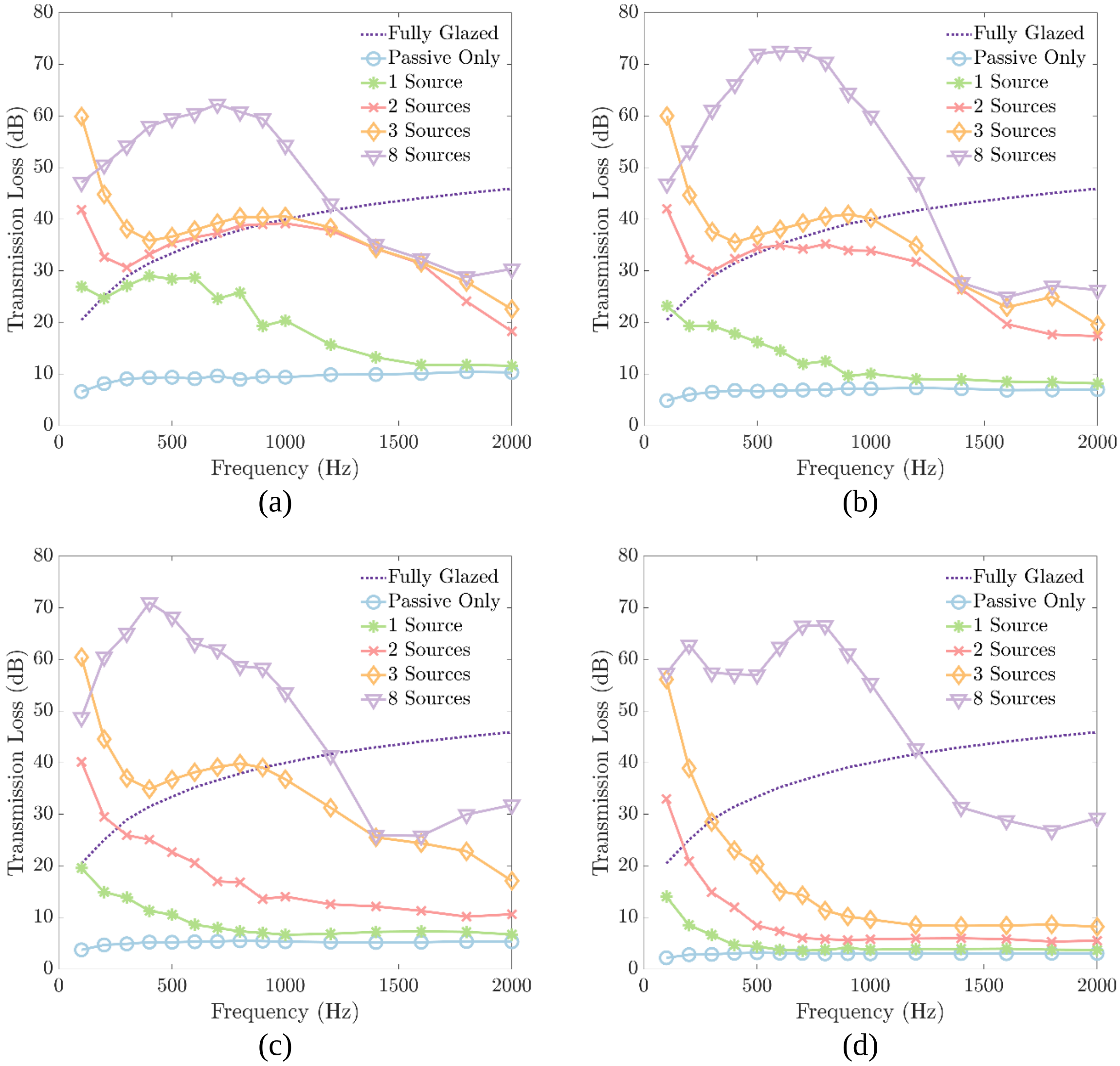

Figure 8: TL of the multiple line source configurations with glazing ratios of (a) 90%, (b) 80%, (c) 70%, and (d) 50%, at 0° noise incidence angle.

By investigating the physical limits of different distributed-layout configurations, the minimum source configuration can be determined for a specific glazing ratio and vice versa. The attenuation performance of different configurations with noise at $\theta = 0^{\circ}$ incidence, is illustrated in Figure 8 for glazing ratio of (a) 90%, (b) 80%, (c) 70%, and (d) 50%. For the numerical simulations of the distributed layout, the position of the N incoherent line sources correspond to the subscript numbering of sources q_N as shown in Figure 7. For instance, one source corresponds to q_1, and three sources are located at positions q_1, q_2, and q_3. The results when N is 1, 2, 3, or 8 are highlighted and compared to the transmission loss of a fully glazed window, and the contributions due to partial glazing without control, as shown in Figure 8.

When there are control sources symmetrically distributed across the entire aperture (i.e., $N = 8$), the transmission loss of the ANC system $TL_{GR,ANC}$ exceeds that of a fully glazed aperture without control TL_1 (purple dashed line), up till 1200 Hz for GR greater than 50%. Although active control with sufficient sources across the entire aperture could ideally yield greater attenuation performance than a fully glazed aperture, it is still worthwhile to determine the minimum configuration that can yield sufficient attenuation for sustainability and practicality.

To achieve similar attenuation as the fully glazed aperture, a minimum of 2 sources are required when the glazing ratio is 90% or less, for frequencies less than 1000 Hz, as shown in Figure 8(a). If the benchmark is lowered to 20 dB, a minimum of 2 sources is required for 70% glazing.

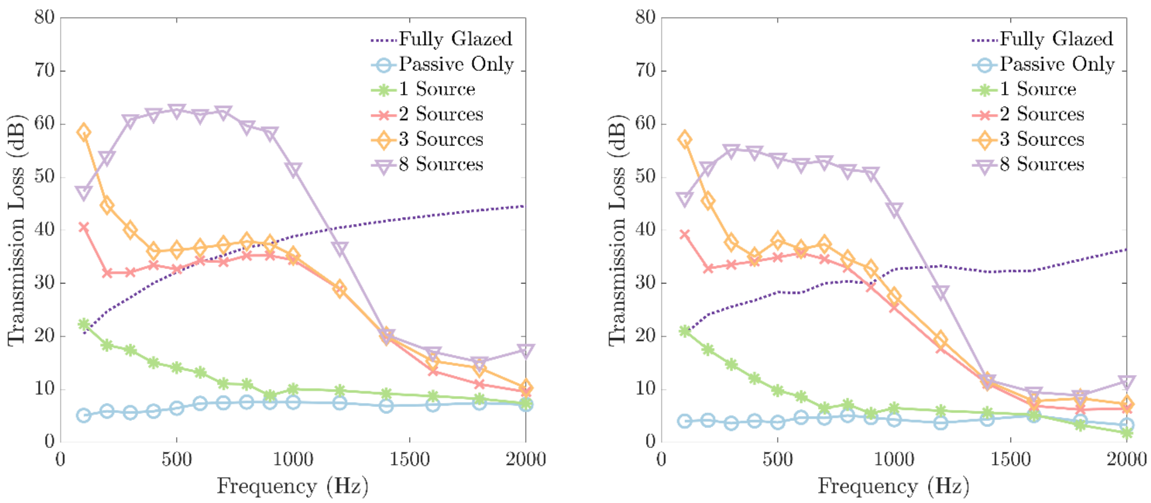

(a) (b)

Figure 9: $TL_{GR,ANC}$ **of** $N = 1, 2, 3,$ and 8 **source configurations at 80% glazing for noise incidence angles at (a)** $30°$**, and (b)** $90°$**.**

The minimum number of sources with respect to the opening size L_o, can be further generalised to $N_{\min} = L_o / w$, where w is predetermined based on the general rule [18]. At a separation of $w = 0.125$ m, the ANC system would be effective up to 2500 Hz at $0°$ incidence and up to half that frequency at $90°$, which would be sufficient to tackle traffic noise [29].

3.4.1 Performance at different angles of incidence

In the 2D simulation model shown in Figure 9, the angle of incidence refers to the azimuthal angles, for instance, from a moving noise source in the horizontal plane. This is analogous to a top-view cross-section of a domestic sliding window. Since the glass panel in the aperture is asymmetric, the angles of incidence are simulated from $\theta = -90°$ to $90°$.

When the noise is normally incident, the performance of both two and three source configurations at glazing ratio of 80%, sufficiently satisfy the benchmark of the fully glazed system, as shown in Figure 8. At glazing ratio of 80% the $TL_{0.8.ANC}$ of the two and three source configurations also satisfy the benchmark as shown in Figure 9 for incidence angles of (a) $30°$, (b) $90°$. The attenuation performance of the corresponding negative noise incidence angles are similar to the positive ones. Since the performance of the two-source system closely matches that of the three sources, it suggests that two sources at 80% glazing can sufficiently attenuate noise at least as well as full glazing at all incidences θ.

4 Experiments

4.1 Test chamber

A $2 \times 2 \times 2$ m^3 wooden chamber was constructed and placed in a recording studio, as depicted in Figure 10. The wooden chamber consists of five 30 mm and one 36 mm thick plywood panels, with the thickest panel housing the window structure and facing the noise source.

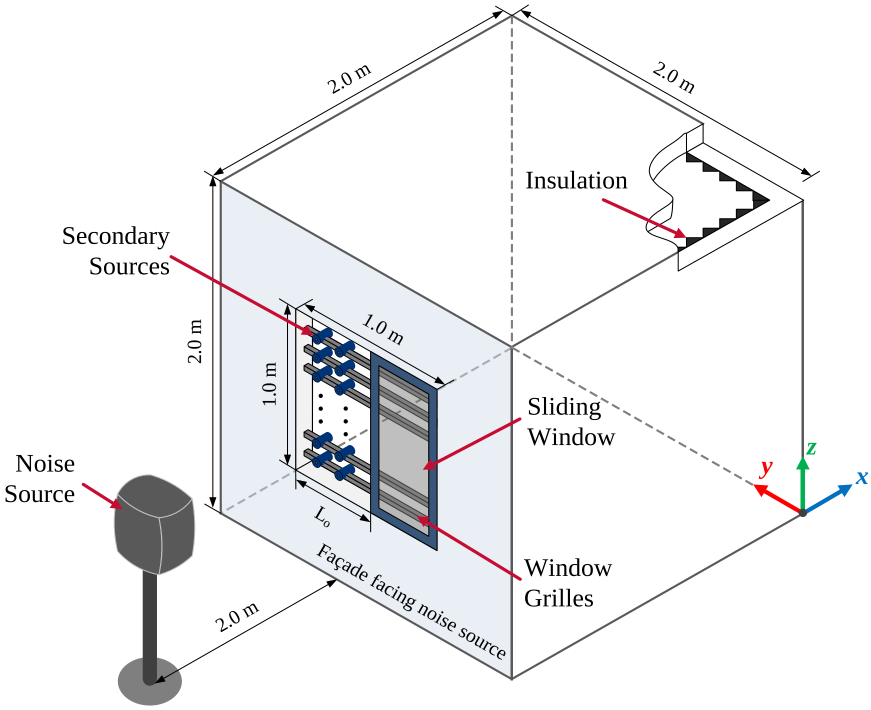

Figure 10: A sketch of the experimental setup with dimensions in m.

A 1×1 m^2 sliding window is installed in the aperture, accompanied by a security grille. The window and grille conform to the standards for domestic windows set by the Singapore standards body, SPRING Singapore [30]. After discounting the frames of the window and grilles, the effective open area of the two-panel sliding window is $(0.93 / 2) \times 0.93$ m^2, where the shorter edge represents the width and the latter representing the height.

To minimise the interference due to reverberation, the inside surface of the entire chamber has been lined with acoustic foam. The opening size is depicted by L_o and the noise source is located 2 m away from the middle of the opening.

4.2 Real-time Active Noise Control System

The primary source is a large loudspeaker (Genelec 8341A) with flat frequency response and large wave fronts. Sixteen secondary sources were installed on the window grille in two columns of 8 sources facing into the chamber, as shown in Figure 11. Taking reference from

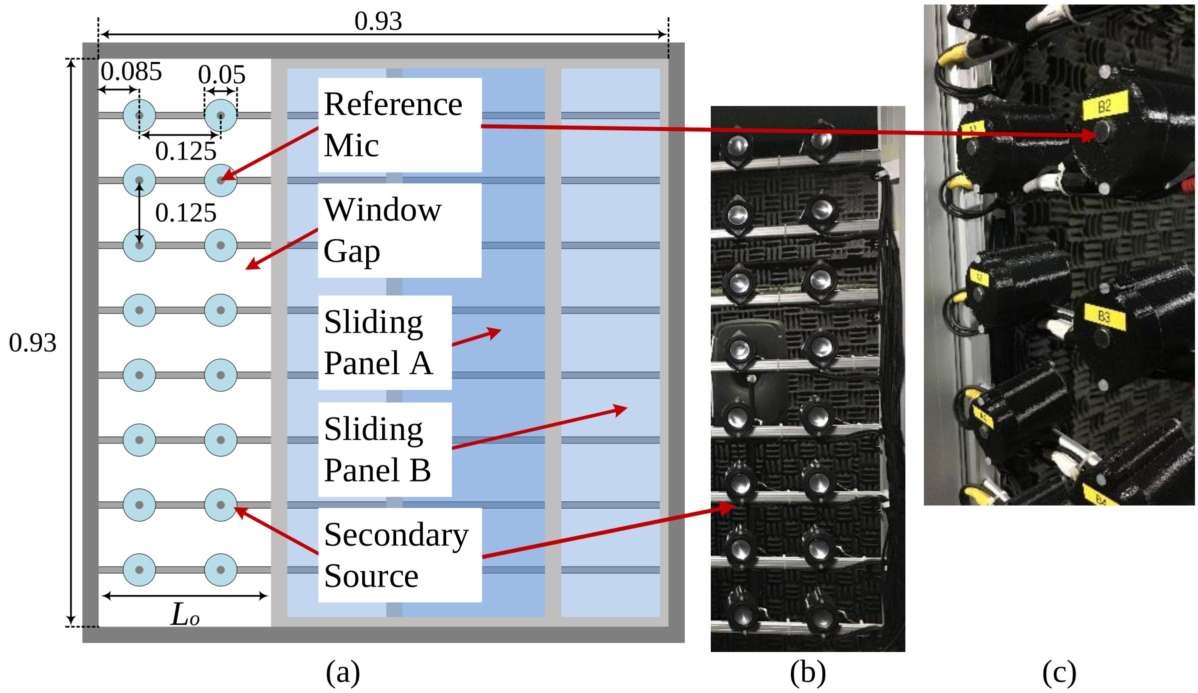

Figure 11: (a) View of the ANC system from outside the chamber with dimensions in m. The secondary source is fixed on the window grille, and L_o is varied by moving sliding panel A only. View of the (b) secondary sources from inside the chamber, and (c) reference microphones from outside.

the Active Acoustic Shielding (AAS) cell proposed by Murao and Nishimura [11], one reference microphone is paired with a secondary speaker to form a single compact unit, as shown in Figure 11(b).

Eight error sensors are placed 0.5 m away from the secondary source to avoid the near-field effects of the secondary sources. There are 27 observation microphones (G.R.A.S. 40PH) distributed inside the chamber, as shown in Figure 12 in both the *xz*-plane (left) and *xy*-plane (right). The observation microphone output from the National Instruments 9234 data acquisition device was analysed with the LabVIEW software.

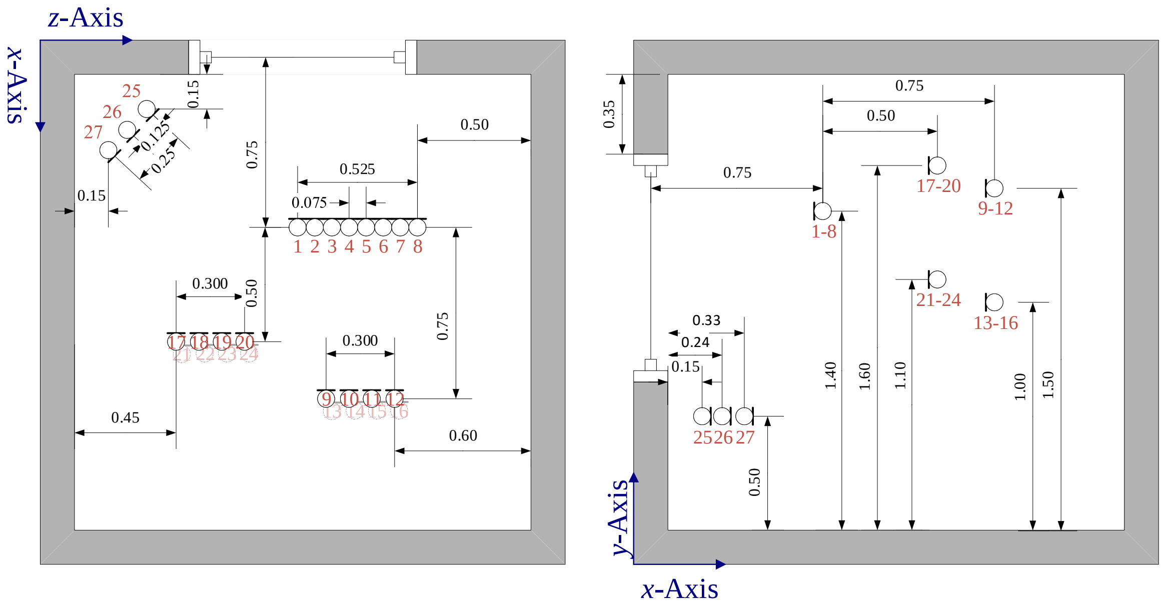

Figure 12. Layout of the 27 observation microphones in the chamber in the *xz*-plane (left) and *xy*-plane (right).

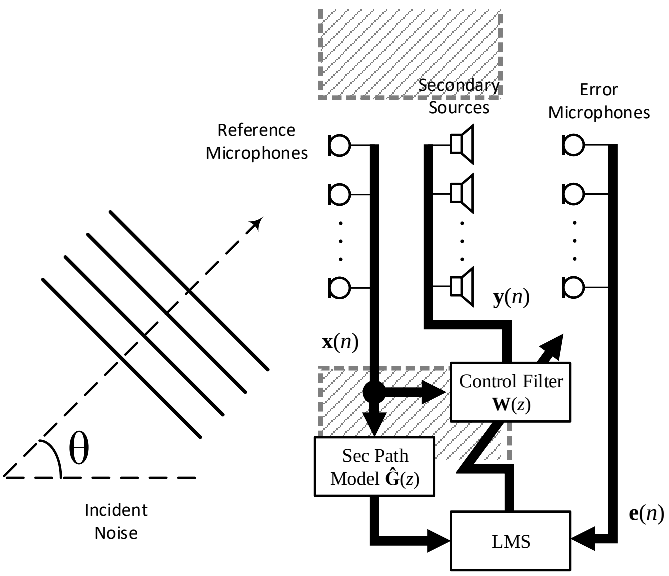

Figure 13: Active control system block diagram showing the cross-section of the physical layout and path of the reference $x(n)$, control $y(n)$, and error $e(n)$ signals. The control filter is updated by the FXLMS algorithm.

A collocated implementation of the FXLMS algorithm [11], was programmed into a modular real-time embedded platform (National Instruments PXIe-8135). The sampling rate was 16 kHz, and the filter lengths of the secondary path model and adaptive filter was set to 100 and 200 taps, respectively. The block diagram of the multichannel ANC system is depicted in Figure 13.

4.3 Evaluation Criteria

The time-averaged SPL readings from all n observation microphones, $SPL_{TA,n}$, are used to determine SPL_{EA} the energy-average sound pressure level in the chamber, given by

$$SPL_{EA} = 10\lg\left(\frac{1}{n}\sum_{i=1}^{n}10^{SPL_{TA,i}/10}\right). \quad (6)$$

The energy-average SPL, SPL_{EA}, represents the space and time average of the SPL in the chamber as defined in ISO 16283-3.

The attenuation of the fully-glazed (*FG*) window as compared to the case where the window gap is L_o m, is thus given by,

$$ATT_{L_o,FG} = SPL_{EA,L_o} - SPL_{EA,FG}, \quad (7)$$

where SPL_{EA,L_o} is the energy-average SPL when the window gap is L_o m, and $SPL_{EA,FG}$ is the energy-average SPL of the fully-glazed system under the same test signal. The attenuation performance of the ANC system is evaluated by

$$ATT_{L_o,ANC} = SPL_{EA,L_o} - SPL_{EA,L_o,ANC}, \quad (8)$$

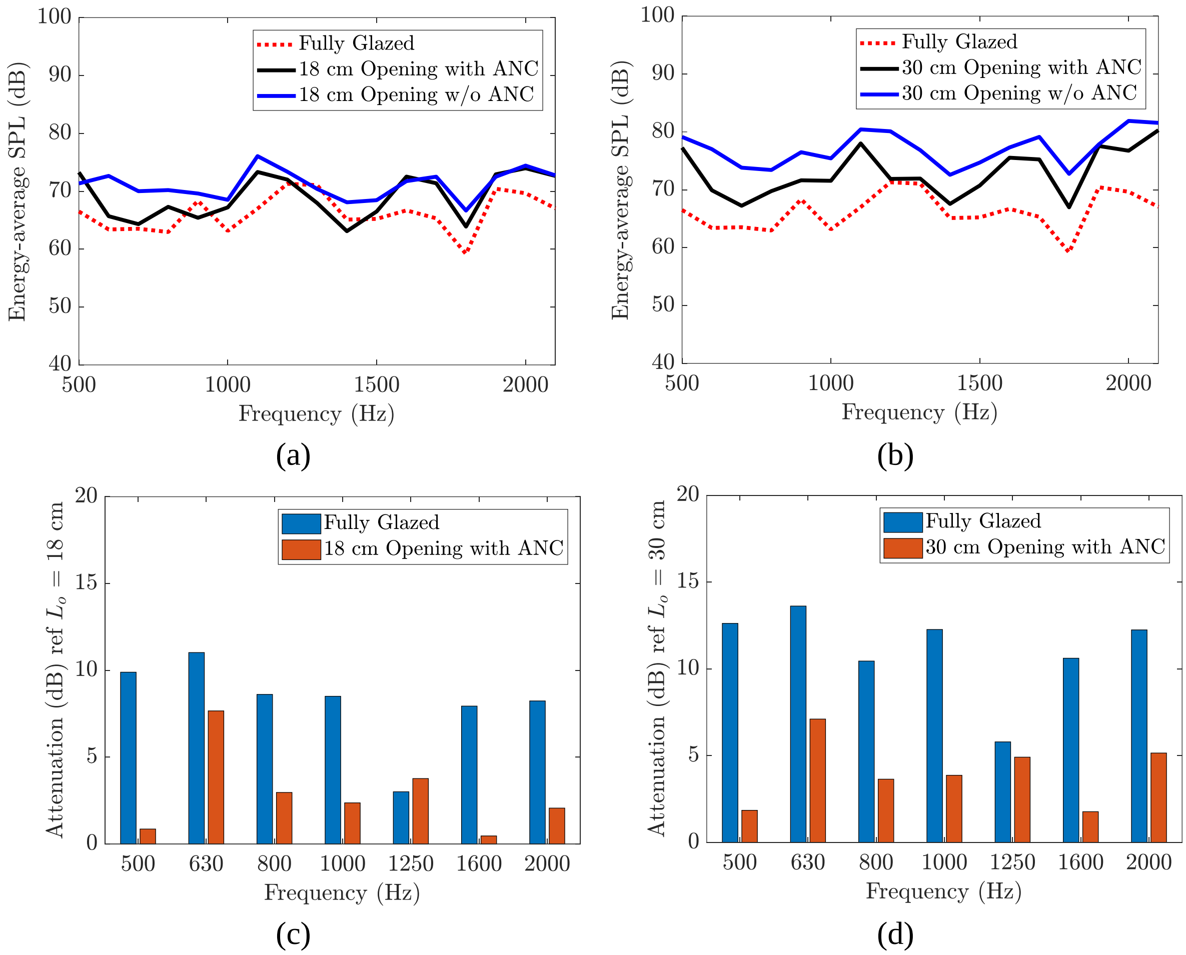

Figure 14. Energy-average sound pressure levels of 27 microphones at (a) $L_o = 0.18$ m **and (b)** $L_o = 0.30$ m**, when (1) fully glazed (red dashed line), (2) without ANC (solid blue line), and (3) with ANC activated (solid black line). Attenuation performance in 1/3 octave bands of the fully-glazed window and an (c) 8-channel and (d) 16-channel ANC system, normalised by the energy-average SPL.**

where $SPL_{EA,L_o,ANC}$ is the energy-average SPL when the window gap is L_o m with ANC activated.

4.4 Test of tonal noise

In the single tone tests, the primary source is excited with frequencies of 500 Hz to 2100 Hz under three scenarios, namely: (1) fully-glazed window, (2) window with glazing ratio GR without active control, and (3) window with glazing ratio GR and active control activated.

When the window is 0.18 m ajar ($L_o = 0.18$ m, $GR \approx 80\%$) the energy-average sound pressure level, $SPL_{EA,L_o=0.18}$ is nearly constant (71 dB ± 2 dB) as reflected by the blue line in Figure 14**Error! Reference source not found.**(a). Shutting the window clearly yields noticeable attenuation as shown by the red dashed line. The layout of the 8-channel system used when $L_o = 0.18$ m is depicted by the left most column of sources in Figure 11(a). Notable attenuation between the 630 to 1250 Hz 1/3 octave bands is achieved with the 8-channel ANC system as indicated by the red bars in **Error! Reference source not found.** Figure 14(c).

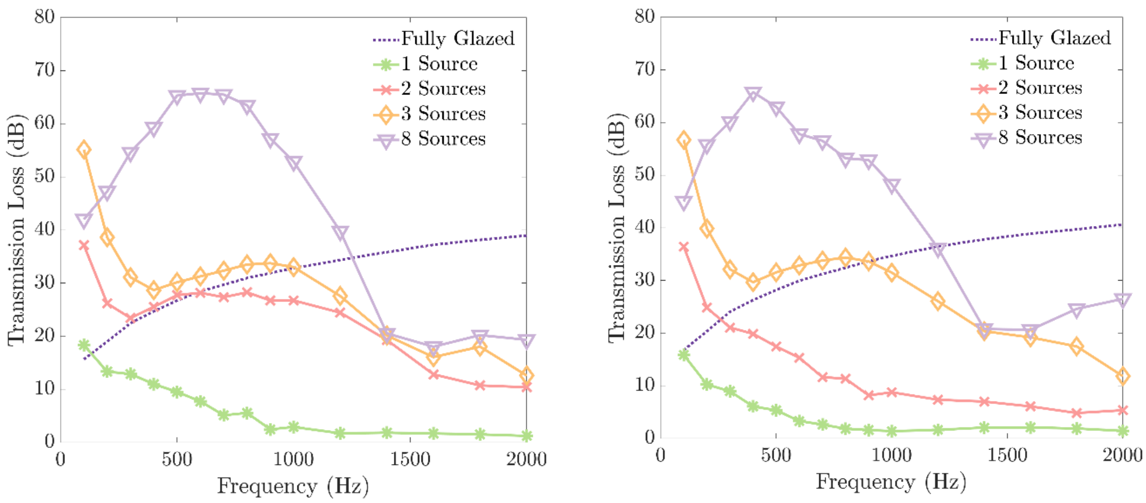

(a) (b)

Figure 15. TL **of the fully-glazed window without ANC, and** TL **of the different source configurations at** GR **of (a) 80%, and (b) 70%, normalised by the sum-of-the-square pressures at the evaluation arc without ANC for** GR **of (a) 80%, and (b) 70%.**

The attenuation performance of the fully-glazed window ($ATT_{L_o,FG}$) and the 8-channel ANC system ($ATT_{L_o,ANC}$) when $L_o = 0.18$ m represented by the blue bars in Figure 14**Error! Reference source not found.**(c). It is expected that the performance of the ANC system would be less effective than the fully-glazed window as discovered in the numerical simulations for the normalised single source performance in Figure 15(a). However, the perceivable reduction is at most 5 dB lower than the fully-glazed window in most frequencies below 1500 Hz, instead of more than 15 dB difference in the FEM simulations in Figure 15(a). This discrepancy arises from both the active control system and the window structure. Despite the inclusion of sealing foam, the passive attenuation of a closed two-panel sliding window is still hampered by the gaps between the panels and the sliding tracks. After optimisation of the secondary source locations, the active control performance is still dependent on the cost function choice, error sensor arrangement, and controller and hardware choices [31].

When the opening L_o is increased to 0.3 m ($GR \approx 70\%$), a 16-channel ANC system is activated. A diagram of the source placement and the actual image, as shown from the inside of the chamber, are depicted in Figure 11. The energy-average SPL in the chamber is significantly increased when the opening is two-thirds wider as shown by the solid blue line in the bottom-left plot in Figure 14**Error! Reference source not found.**(b). Considerable passive noise reduction (<10 dB) is achieved when the window is fully glazed (dashed red line). Between 630 to 1250 Hz 1/3 octave bands, the attenuation performance of the 16-channel ANC system is better than the performance of the 8-channel system when $L_o = 18$ cm, as shown in Figure 14**Error! Reference source not found.**(d).

5 Discussion

It is expected from the simulations that the performance of the active control system will be worse than the passive attenuation of a fully-glazed system. However, the difference between both ANC configurations and the fully-glazed system is only between 5 to 10 dB (energy-average SPL) in most frequencies below 1500 Hz, in contrast to the sound power difference of greater than 15 dB in the finite element simulations.

Even though the (demonstrated) system has a large opening similar to actual in-situ usage, and larger than that demonstrated by Murao and Nishimura, Carme et al., and Kwon and Park, the performance trade-offs have to be addressed.

In the proposed system, the size of the speaker diaphragm was reduced (0.045 m) in favour of reduced visual obstruction. Hence, the low frequency performance (<500 Hz) was drastically affected. Depending on the target noise, however, there may not be a need to address this shortcoming as the dominant energy is usually not less than 500 Hz (i.e., traffic noise) and human hearing is less sensitive to low frequencies.

To realise the active control system for practical applications, the high computational complexity associated with the implementation of the multi-channel system needs to be addressed [32–34]. Moreover, development of a computationally efficient method, as opposed to regular leaky FXLMS, is required to prevent overdriving the control sources in the presence of high SPL noise especially for small speakers [35]. Further investigation into the robustness of the fixed coefficient implementation allows for the omission of error microphones in the interior of the room [36–38], a major boon for practical implementation.

6 Conclusion

To establish a performance benchmark for the active control of noise through open windows, the transmission loss of a single-glazed aperture was investigated through FEM simulations. The simulations represent an ideal glazing scenario, where the glass panel is perfectly sealed to the rigid walls.

The physical limits of two types of control source arrangements and their interactions with varying glazing ratios were examined. In the ideal control scenario, the distributed control source method consistently outperforms the boundary control method for different glazing ratios and angles of plane noise incidence.

A guideline is formulated for realising a practical ANC system on standard windows in Singapore through investigation of the physical limits of control, for an increasing number of control sources in the distributed configuration at different glazing ratios and angles of incidences. The recommended window gap should be guided by the minimum source separation distance determined for sufficient control of traffic noise, where $N_{min} = L_o / w$ and $w = 0.125$ m.

A full-scale model with an actual domestic sliding window and security grille was constructed to test the performance of the distributed control system. Although it was determined that at 80% glazing, two sources (line) would sufficiently attain the attenuation performance of a fully-glazed window, it is not realisable in practical conditions due to the partial obstruction of reference microphones on the proposed control cell. After accounting for the physical constraints of the real window, two distributed configurations were tested, (1) 8 sources arranged uniformly in a vertical column in a 0.1674 m^2 opening ($0.18 \times 0.93\ \mathrm{m}^2$, $GR = 0.8$), and (2) 16 sources arranged uniformly in two vertical columns in a 0.279 m^2 opening ($0.3 \times 0.93\ \mathrm{m}^2,\ GR = 0.7$).

Through tonal experiments, notable attenuation (> 5 dB energy-average SPL) was achieved by means of a 16-channel ANC system installed in real window at 70% ($0.3 / (0.93 \times 0.465)$ m^2) of its maximum allowable opening size.

Acknowledgement

This material is based on research/work supported by the Singapore Ministry of National Development and National Research Foundation under L2 NIC Award No.: L2NICCFP1-2013-7

References

[1] J. Kang, An acoustic window system with optimum ventilation and daylighting performance, Noise Vib. Worldw. 37 (2009) 9–17. doi:10.1260/095745606779385108.

[2] Y.G. Tong, S.K. Tang, Plenum window insertion loss in the presence of a line source—A scale model study, J. Acoust. Soc. Am. 133 (2013) 1458–1467. doi:10.1121/1.4788996.

[3] Y.G. Tong, S.K. Tang, J. Kang, A. Fung, M.K.L. Yeung, Full scale field study of sound transmission across plenum windows, Appl. Acoust. 89 (2015) 244–253. doi:10.1016/j.apacoust.2014.10.003.

[4] H. Huang, X. Qiu, J. Kang, Active noise attenuation in ventilation windows., J. Acoust. Soc. Am. 130 (2011) 176–88. doi:10.1121/1.3596457.

[5] X. Qiu, H. Huang, Z. Lin, Progress in research on natural ventilation ANC windows, in: INTER-NOISE NOISE-CON Congr. Conf. Proc., Institute of Noise Control Engineering, 2011: pp. 3189–3196.

[6] H.M. Lee, L.B. Tan, K.M. Lim, H.P. Lee, Experimental study of the acoustical performance of a sonic crystal window in a reverberant sound field, Build. Acoust. (2016) 1351010X16681015. doi:10.1177/1351010X16681015.

[7] B. Kwon, Y. Park, Interior noise control with an active window system, Appl. Acoust.

74 (2013) 647–652. doi:10.1016/j.apacoust.2012.11.005.

[8] T. Pàmies, J. Romeu, M. Genescà, R. Arcos, Active control of aircraft fly-over sound transmission through an open window, Appl. Acoust. 84 (2014) 116–121. doi:10.1016/j.apacoust.2014.02.018.

[9] C. Carme, O. Schevin, C. Romerowski, J. Clavard, Active Noise Control Applied to Open Windows, in: INTER-NOISE NOISE-CON Congr. Conf. Proc., Hamburg, Germany, 2016: pp. 3058–3064.

[10] J. Hanselka, S. Jukkert, D. Sachau, Experimental Study on the Influence of the Sensor and Actuator Arrangement on the Performance of an Active Noise Blocker for a Tilted Window, in: INTER-NOISE NOISE-CON Congr. Conf. Proc., Hamburg, Germany, 2016: pp. 3046–3057.

[11] T. Murao, M. Nishimura, Basic Study on Active Acoustic Shielding, J. Environ. Eng. 7 (2012) 76–91.

[12] T. Murao, M. Nishimura, K. Sakurama, S. Nishida, Basic study on active acoustic shielding (Improving noise-reducing performance in low-frequency range), Mech. Eng. J. 1 (2014) EPS0065-EPS0065. doi:10.1299/mej.2014eps0065.

[13] J. Tao, S. Wang, X. Qiu, J. Pan, Performance of an independent planar virtual sound barrier at the opening of a rectangular enclosure, Appl. Acoust. 105 (2016) 215–223. doi:10.1016/j.apacoust.2015.12.019.

[14] S. Wang, J. Tao, X. Qiu, Performance of a planar virtual sound barrier at the baffled opening of a rectangular cavity, J. Acoust. Soc. Am. 138 (2015) 2836–2847. doi:10.1121/1.4934267.

[15] S. Wang, J. Yu, X. Qiu, M. Pawelczyk, A. Shaid, L. Wang, Active sound radiation control with secondary sources at the edge of the opening, Appl. Acoust. 117 (2017) 173–179. doi:10.1016/j.apacoust.2016.10.027.

[16] S. Elliott, J. Cheer, B. Lam, C. Shi, W. Gan, Controlling Incident Sound Fields With Source Arrays in Free Space and Through Apertures, in: B.M. Gibbs (Ed.), Proc. 24th Int. Congr. Sound Vib., London, UK, 2017: pp. 1–7.

[17] C. Carme, O. Schevin, C. Romerowski, J. Clavard, Active opening windows, in: Proc. 23rd Int. Congr. Sound Vib. ICSV23, Athens, Greece, 2016.

[18] B. Lam, S. Elliott, J. Cheer, W.-S. Gan, Physical limits on the performance of active noise control through open windows, Appl. Acoust. 137 (2018) 9–17. doi:10.1016/j.apacoust.2018.02.024.

[19] S. Wang, J. Tao, X. Qiu, Controlling sound radiation through an opening with secondary loudspeakers along its boundaries, Sci. Rep. 7 (2017) 13385. doi:10.1038/s41598-017-13546-2.

[20] S.J. Elliott, J. Cheer, B. Lam, C. Shi, W. Gan, A wavenumber approach to analysing the active control of plane waves with arrays of secondary sources, J. Sound Vib. 419 (2018) 405–419. doi:10.1016/j.jsv.2018.01.028.

[21] X. Yu, S.-K. Lau, L. Cheng, F. Cui, A numerical investigation on the sound insulation of ventilation windows, Appl. Acoust. 117 (2017) 113–121. doi:10.1016/j.apacoust.2016.11.006.

[22] J.D. Quirt, Sound transmission through windows I. Single and double glazing, J. Acoust. Soc. Am. 72 (1982) 834–844. doi:doi:http://dx.doi.org/10.1121/1.388263.

[23] A.J.B. Tadeu, D.M.R. Mateus, Sound transmission through single, double and triple glazing. Experimental evaluation, Appl. Acoust. 62 (2001) 307–325. doi:http://dx.doi.org/10.1016/S0003-682X(00)00032-3.

[24] A. Tadeu, A. Pereira, L. Godinho, J. António, Prediction of airborne sound and impact sound insulation provided by single and multilayer systems using analytical expressions, Appl. Acoust. 68 (2007) 17–42. doi:http://dx.doi.org/10.1016/j.apacoust.2006.05.012.

[25] S.J. Elliott, Signal Processing for Active Control, Academic Press, London, UK, 2001. http://www.sciencedirect.com/science/book/9780122370854 (accessed May 9, 2017).

[26] COMSOL Multiphysics, Acoustics Module User's Guide, (2015).

[27] W.P. Rdzanek, Sound scattering and transmission through a circular cylindrical aperture revisited using the radial polynomials, J. Acoust. Soc. Am. 143 (2018) 1259–1282. doi:10.1121/1.5025159.

[28] B. Lam, S.J. Elliott, J. Cheer, W.-S. Gan, The Physical Limits of Active Noise Control of Open Windows, in: K.M. Lim (Ed.), Proc. 12th West. Pacific Acoust. Conf., Singapore, 2015: pp. 184–189.

[29] A. Jagniatinskis, B. Fiks, Assessment of environmental noise from long-term window microphone measurements, Appl. Acoust. 76 (2014) 377–385. doi:http://dx.doi.org/10.1016/j.apacoust.2013.09.007.

[30] SPRING (Standards Productivity and Innovation Board) Singapore, Specification for aluminium alloy windows, 4th Rev., Singapore, 2007.

[31] C. Hansen, S. Snyder, X. Qiu, L. Brooks, D. Moreau, Active Control of Noise and Vibration, Second Edition, CRC Press, 2012.

[32] T. Murao, C. Shi, W.-S. Gan, M. Nishimura, Mixed-error approach for multi-channel active noise control of open windows, Appl. Acoust. 127 (2017) 305–315. doi:10.1016/j.apacoust.2017.06.024.

[33] D. Shi, C. Shi, W.-S. Gan, A systolic FxLMS structure for implementation of feedforward active noise control on FPGA, in: 2016 Asia-Pacific Signal Inf. Process. Assoc. Annu. Summit Conf., IEEE, 2016: pp. 1–6. doi:10.1109/APSIPA.2016.7820755.

[34] D. Shi, J. He, C. Shi, T. Murao, W.-S. Gan, Multiple parallel branch with folding architecture for multichannel filtered-x least mean square algorithm, in: 2017 IEEE Int. Conf. Acoust. Speech Signal Process., 2017.

[35] D. Shi, B. Lam, W.-S. Gan, A novel selective active noise control algorithm to overcome practical implementation issue, in: 2018 IEEE Int. Conf. Acoust. Speech Signal Process., IEEE, Calgary, Canada, 2018: pp. 1–5.

[36] K. Tanaka, C. Shi, Y. Kajikawa, Binaural active noise control using parametric array loudspeakers, Appl. Acoust. 116 (2017) 170–176. doi:10.1016/J.APACOUST.2016.09.021.

[37] B. Lam, J. He, T. Murao, C. Shi, W.-S. Gan, S.J. Elliott, Feasibility of the full-rank fixed-filter approach in the active control of noise through open windows, in: INTER-NOISE NOISE-CON Congr. Conf. Proceedings, InterNoise16, Hamburg, Germany, 2016: pp. 3548–3555.

[38] R. Ranjan, J. He, T. Murao, B. Lam, W.-S. Gan, Selective Active Noise Control System for Open Windows using Sound Classification, in: INTER-NOISE NOISE-CON Congr. Conf. Proceedings, InterNoise16, Hamburg, Germany, 2016: pp. 482–492.